Mitochondrial dysfunction associated with viral cytopathogenicity

Mais G. Ammari[1,3], G. Todd Pharr[1], Matthew K. Ross[1], George V. Pinchuk[2] and Lesya M. Pinchuk[1,*]

[1]Department of Basic Sciences, Mississippi State University, Mississippi State, MS 39762, USA,
[2]Department of Sciences and Mathematics, Mississippi University for Women, Columbus, MS 39701, USA, [3]School of Animal and Comparative Biomedical Sciences, University of Arizona, Tucson, AZ 85721, USA

ABSTRACT

The mitochondria play a vital role in one of the major apoptosis signalling pathways. Dysfunction in the mitochondria is crucial in the pathogenesis of several viral diseases. In the case of Bovine Viral Diarrhea Virus (BVDV), the cytopathic (CP) biotype, but not the non-cytopathic (NCP) biotype is implicated in the induction of apoptosis. Using state-of-the-art proteomics we demonstrated that bovine monocytes infected with CP BVDV exhibited strong down-regulation of proteins involved in mitochondrial functions, including oxidative phosphorylation- (OxPhos) and the antioxidant catalase (CAT) proteins. In this study, we further assessed the mechanisms of BVDV-induced apoptosis in a susceptible bovine turbinate (BT) cell line by using multiple functional flow cytometry approaches. We demonstrate the direct involvement of CP BVDV but not the NCP counterpart in mitochondrial membrane potential ($\Delta\Psi$m) disruption and generation of reactive oxygen species (ROS) in infected BT cells. Our data show that CP BVDV contributed to oxidative stress by significantly decreasing the expression of cellular antioxidant enzyme peroxiredoxin1 (PRDX1) and numerically decreasing the levels of CAT. We confirm and extend our proteome findings that the direct damage to mitochondrial proteins decreases their function and contributes to $\Delta\Psi$m breakdown and the hyperproduction of ROS seen in BT cells infected with CP but not with NCP BVDV. Overall, our data show that CP and NCP BVDV differentially target mitochondrial proteins and antioxidant enzymes that control the fate of infected cells and determine whether BVDV produces cytopathic effects or replicate non-cytopathically to establish persistent infection.

INTRODUCTION

Over the years, viruses from several genera and families have evolved multiple strategies to elicit oxidative stress and trigger apoptotic cell death [1-8]. These viruses cause an up-regulation in the expression of certain proteins that serve as inducers of apoptosis and also down-regulate proteins that normally have an anti-apoptotic function. An important model in studies of virus-induced apoptosis is Bovine Viral Diarrhea Virus (BVDV). BVDV is a small enveloped positive single-stranded RNA virus classified in the family *Flaviviridae* [9, 10]. Based on their cytopathogenicity in cultured cells, BVDV falls into two biotypes: non-cytopathic (NCP) and cytopathic (CP). While the NCP biotype fails to induce apoptosis [11], the CP biotype induces

*Corresponding author: pinchuk@cvm.msstate.edu

cellular responses mainly implicated in the induction of an intrinsic pathway of apoptosis [12-15], a pathway which is known to be triggered by mitochondrial dysfunction [16, 17].

Previously, Grummer and co-workers showed that incubation of fetal bovine kidney (FBK) cells with mitochondrial permeability transition pore (MPTP) inhibitors delayed the cytopathic effect of BVDV-1. The authors suggested that a breakdown in mitochondrial membrane potential ($\Delta\Psi$m) and increased caspase-9 activity with subsequent release of cytochrome *c* from the mitochondria were involved in apoptosis of BVDV-1-infected fetal bovine kidney (FBK) cells [15]. Schweizer and Peterhans demonstrated that the generation of reactive oxygen species (ROS) is a prominent feature of BVDV-induced apoptosis and occurs earlier than other apoptotic signs [12]. Furthermore, it was shown that initiation of apoptosis correlated with the down-regulation of antiapoptotic Bcl-2 protein and decreased glutathione levels, thereby inducing endoplasmic reticulum stress-mediated apoptosis in Madin-Darby Bovine Kidney (MDBK) cells [14]. They also showed that ROS generated in MDBK cells infected with CP biotype can activate poly ADP-ribose polymerase (PARP), a nuclear enzyme involved in DNA repair [18]. These studies demonstrated that the cytopathic effect of CP BVDV in various cell types is attributed mainly to the intrinsic pathway of apoptosis. However, the mechanisms are not well understood at this stage.

Lambot and co-workers showed that cells undergoing apoptosis, due to CP BVDV-infection, were predominantly found in the monocyte population of bovine peripheral blood mononuclear cells (PBMC) that contributed to the induction of T cell death [19]. In our previous proteomics study, we identified differentially expressed proteins significantly altered in bovine monocytes after 24 hrs infection with CP or NCP BVDV compared to uninfected controls [20]. We identified the top immunological pathways involved in each infection using Ingenuity Pathway Analysis (IPA; Ingenuity system, CA). To further investigate the mitochondria-related apoptosis in BVDV-infected monocytes, we conducted an additional analysis of the differentially expressed host proteins [20] using IPA to visualize pathways that are affected by infection with CP

and NCP BVDV biotypes. Our results show that CP BVDV differentially affected proteins in multiple mitochondrial-related pathways by significantly decreasing their expression levels compared to the NCP BVDV biotype that affected a fewer number of proteins, by mostly enhancing their expression (Table 1). Proteins that are altered due to BVDV infection in oxidative phosphorylation (OxPhos) system are shown in Table 2 with respect to the complexes involved in this pathway. The involvement of the antioxidant enzymes are shown in Table 3. The purpose of this study was to further characterize the mechanisms of BVDV-dependent mitochondrial dysfunction by assessing the similarities and differences between two BVDV-susceptible cell types: primary monocytes and cultured embryotic BT cells [21, 12]. Using multiple approaches we show that the apoptosis caused by the CP, but not the NCP BVDV, induces a dysfunction in mitochondria and an oxidative stress cell death in infected primary and BT cells.

MATERIALS AND METHODS

Cells and viruses

BVDV-free BT cell line was obtained from the American Type Culture Collection (ATCC) and propagated in Dulbecco Minimal Essential Media (DMEM, Invitrogen) supplemented with 2 mM L-glutamine, 1.5 g/l sodium bicarbonate, 50 µg/ml gentamicin and 10% fetal bovine serum (FBS) at 37 °C in 5% CO_2.

BVDV biotypes were prepared as described elsewhere [12]. Briefly, the CP BVDV biotype NADL was obtained from the ATCC and amplified by growing in the BT cell line according to the manufacturer's handling procedures. The infectivity of the NADL biotype was measured using the quantal method of Reed and Muench and the tissue culture infectious dose 50 ($TCID_{50}$) was determined. For the non-cytopathic (NCP) BVDV biotype NY, we used the $TCID_{50}$ suggested by the manufacturer (ATCC).

In the following assays, BT cells were infected at a multiplicity of infection (MOI) of 0.2 with CP or NCP BVDV for 1, 12, 24, 36 and 48 hrs. Uninfected cells at each time point were used as a negative control. At the indicated time point, cells were detached

Table 1. Proteins significantly altered in monocytes after CP or NCP BVDV infections and their corresponding pathways*.

Pathway	Host proteins altered due to	
	CP BVDV infection	NCP BVDV infection
Mitochondrial dysfunction	AIFM1, ATP5A1, ATP5B, ATP5C1, CAT, COX5A, CPT1A, CYB5R3, GPD2, HSD17B10, MAOA, NDUFA5, **NDUFB7**, NDUFS4, OGDH, PDHA1, **SOD2**	**NDUFB7, PRDX5, SOD2, UCP2**
Propanoate metabolism	ACAA1, ACADSB, ACAT1, ACSF3, ACSS1, ALDH2, ALDH4A1, HADHA, IVD, PCCA, SUCLG1, SUCLG2	**ACAT2,** ACSF3, ACSS1, **ALDH5A1, SDS**
Valine, Leucine and Isoleucine degradation	ACAT1, ACAA1, ACAA2, ACADSB, ALDH2, ALDH4A1, HADHA, HSD17B10, IVD, PCCA	**ACAT2, ALDH5A1, SDS**
Pyruvate metabolism	ACAA1, ACAT1, ACSS1, ALDH2, ALDH4A1, HADHA, MDH1, PCK2, PDHA1, PDHB	**ACAT2,** ACSS1, **ALDH5A1, PKM2**
Citrate cycle	IDH2, IDH3A, MDH1, OGDH, PCK2, SUCLG1, SUCLG2	
Butanoate metabolism	ACAA1, ACAT1, ALDH2, ALDH4A1, HADHA, HSD17B10, PDHA1, PDHB, SUCLG2	**ACAT2, ALDH5A1, SDS**
Oxidative phosphorylation	ATP5A1, ATP5B, ATP5C1, ATP5F1, ATP5I, ATP5O, **ATP6V1A,** COX5A, NDUFA5, **NDUFB7,** NDUFC2, NDUFS4	**ATP6V1A, NDUFB7**
Fatty acid metabolism	ACAA1, ACAA2, ACADSB, ACAT1, ALDH2, ALDH4A1, CPT1A, DCI, HADHA, HSD17B10, IVD	

Bold and non-bold proteins indicate up-regulation and down-regulation due to BVDV infection compared to uninfected cells proteins, respectively.
ACAA1: acetyl-CoA acyltransferase 1; ACAA2: acetyl-CoA acyltransferase 2; ACADSB: acyl-CoA dehydrogenase, short/branched chain; ACAT1: acetyl-CoA acetyltransferase 1; ACAT2: acetyl-CoA acetyltransferase 2; ACSF3: acyl-CoA synthetase family member 3; ACSS1: acyl-CoA synthetase short-chain family member 1; AIFM1: apoptosis-inducing factor, mitochondrion-associated, 1; ALDH2: aldehyde dehydrogenase 2 family (mitochondrial); ALDH4A1: aldehyde dehydrogenase 4 family, member A1; ATP5A1: ATP synthase, H+ transporting, mitochondrial F1 complex, alpha subunit 1, cardiac muscle; ATP5B: ATP synthase, H+ transporting, mitochondrial F1 complex, beta polypeptide; ATP5C1: ATP synthase, H+ transporting, mitochondrial F1 complex, gamma polypeptide 1; ATP5F1: ATP synthase, H+ transporting, mitochondrial Fo complex, subunit B1; ATP5I: ATP synthase, H+ transporting, mitochondrial Fo complex, subunit E; ATP5O: ATP synthase, H+ transporting, mitochondrial F1 complex, O subunit; ATP6V1A: ATPase, H+ transporting, lysosomal 70kDa, V1 subunit A; CAT: catalase; COX5A: cytochrome c oxidase subunit Va; CPT1A: carnitine palmitoyltransferase 1A (liver); CYB5R3: cytochrome b5 reductase 3; DCI: dodecenoyl-CoA isomerase; GPD2: glycerol-3-phosphate dehydrogenase 2 (mitochondrial); HADHA: hydroxyacyl-CoA dehydrogenase/3-ketoacyl-CoA thiolase/enoyl-CoA hydratase (trifunctional protein), alpha subunit; HSD17B10: hydroxysteroid (17-beta) dehydrogenase 10; IDH2: isocitrate dehydrogenase 2 (NADP+), mitochondrial; IDH3A: isocitrate dehydrogenase 3 (NAD+) alpha; IVD: isovaleryl-CoA dehydrogenase; MAOA: monoamine oxidase A; MDH1: malate dehydrogenase 1, NAD (soluble); NDUFA5: NADH dehydrogenase (ubiquinone) 1 alpha subcomplex, 5, 13kDa; NDUFB7: NADH dehydrogenase (ubiquinone) 1 beta subcomplex, 7, 18kDa; NDUFC2: NADH dehydrogenase (ubiquinone) 1, subcomplex unknown, 2, 14.5kDa; NDUFS4: NADH dehydrogenase (ubiquinone) Fe-S protein 4, 18kDa (NADH-coenzyme Q reductase); OGDH: oxoglutarate (alpha-ketoglutarate) dehydrogenase (lipoamide); PCCA: propionyl CoA carboxylase, alpha polypeptide; PCK2: phosphoenolpyruvate carboxykinase 2 (mitochondrial); PDHA1 (includes EG:5160): pyruvate dehydrogenase (lipoamide) alpha 1; PDHB: pyruvate dehydrogenase (lipoamide) beta; PKM2: pyruvate kinase, muscle; PRDX5: peroxiredoxin 5; SDS: serine dehydratase; SOD2: superoxide dismutase 2, mitochondrial; SUCLG1: succinate-CoA ligase, alpha subunit; SUCLG2: succinate-CoA ligase, GDP-forming, beta subunit; UCP2: uncoupling protein 2 (mitochondrial, proton carrier).
*The data in the table originate from our previous study [20] with further analysis for mitochondrial dysfunction pathways applied.

Table 2. Altered proteins involved in OxPhos pathway complexes in BVDV-infected monocytes*.

	Complex I	Complex II	Complex III	Complex IV	Complex V
CP BVDV-infection	**NDUFB7,** NDUFA5, NDUFC2, NDUFS4	SDHA		COX5A	**ATP6V1A,** ATP5A1, ATP5B, ATP5C1, ATP5F1, ATP5I, ATP5O
NCP BVDV-infection	**NDUFB7**				**ATP6V1A**

Proteins in bold indicates up-regulation and non-bold indicates down-regulation.
*The data in the table originate from our previous study [20] with further analysis for mitochondrial dysfunction pathways applied.

Table 3. Altered antioxidant proteins in BVDV-infected monocytes*.

		Regulation	
Symbol	Description	CP	NCP
CAT	Catalase	Down	
PRDX1	Peroxiredoxin 1		Up
PRDX5	Peroxiredoxin 5, mitochondrial precursor		Up
TXNRD1	Thioredoxin reductase 1	Up	Up
SOD2	Superoxide dismutase 2	Up	Up

*The data in the table originate from our previous study [20] with further analysis for mitochondrial dysfunction pathways applied.

using cell dissociation buffer (Gibco®) and 10^6 cells were incubated with different probes as follows.

Annexin V/Propidum Iodide assays for apoptosis

Apoptosis in BT cells was assessed using Annexin V/Propidium Iodide (PI) detection kit (Invitrogen) as previously described [22]. Briefly, after viral infection, adherent cells were washed twice with phosphate-buffered saline (PBS) and then incubated with Annexin V-FITC and PI (5 ug/ml each) in 1x binding buffer for 10 min at room temperature in the dark. Annexin V detects cells that have expressed phosphatidylserine (PS) on the cell surface, an event found in apoptosis. Cells were analyzed immediately with a flow cytometer (FACSCalibur™, BD Bioscience, San Jose, CA) using two-color analysis with Dot Plot Quadrant Statistics while gating on live cells. Both early apoptotic (Annexin V-positive and PI-negative) and late apoptotic (Annexin V-positive and PI-positive) cells were included in cell death determinations. Cells treated for 1 hr with staurosporine (1 μM, Sigma) were used as a positive control for apoptosis.

Determination of mitochondrial membrane potential

Changes in the mitochondrial membrane potential (ΔΨm) following infection with BVDV biotypes were measured using DePsipherTM staining (R&D systems, Minneapolis, MN). To indicate the loss of mitochondrial membrane potential, the DePsipherTM kit uses a cationic dye (5,5',6,6'-tetrachloro-1,1',3,3'-tetraethylbenzimidazolylcarbocyanine iodide) that possesses the property to aggregate upon membrane polarization forming an orange-red fluorescent compound. In cells with disturbed potential, the reagent cannot accumulate in the mitochondria and remains in the cytoplasm as a green monomeric form. Adherent cells were collected and washed following infection. Cells treated with 1 μM staurosporine for 1 hr served as positive control. Cells were incubated with 5 μg/ml DePsipherTM for 20 min at 37 °C and 5% CO_2 and then washed twice with pre-warmed 1x DePsipher reaction buffer. The percentage of orange and green fluorescence was measured by flow

cytometry according to the manufacturer's instructions. All measurements were done in duplicates with gating on viable cells.

Measurement of reactive oxygen species accumulation

Intracellular reactive oxygen species (ROS) levels were measured using the fluorescent dye carboxy-H_2DCFDA (Invitrogen) staining method as described previously [23]. Briefly, after infection, adherent cells were washed and re-suspended in PBS containing carboxy-H2DCFDA (10 μM) and incubated for 1 hr at 37 °C in the dark. Positive control cells were treated for 1 hr with hydrogen peroxide (H_2O_2) (100 μM). The non-fluorescent dye freely penetrates cells and can be hydrolyzed by intracellular esterases to 2´,7-dichlorodihydrofluororescein (DCFH), which is trapped inside the cells. DCFH converts to fluorescent DCF upon reaction with various ROS like hydroxyl radicals, H_2O_2 and superoxide anions. The mean fluorescent intensity (MFI) of DCF fluorescence was determined as intracellular ROS levels with flow cytometry.

Antioxidant enzymes

For detection of intracellular antioxidant enzymes, cells were fixed and permeabilized using BD Cytofix/Cytoperm Kit (BD Biosciences) solution for 20 min at 4 °C. Cells were then stained with anti-catalase polyclonal antibody (Thermo Scientific) or anti PRDX1 polyclonal antibody (Life Span) for 30 min at 37 °C. Cells were then washed and incubated with the appropriate secondary antibody conjugated with FITC for 30 min at 37 °C. Cells were washed and then analyzed using flow cytometry.

Western blot

Cell lysates were prepared from uninfected or BVDV-infected cells at 1, 12 and 24 hrs post-infection using IP lysis/wash buffer (Pierce). The lysates were resolved by 10% Sodium Dodecyl Sulfate Poly-Acrolamide Gel Electrophoresis (SDS-PAGE) and transferred to nitrocellulose membranes. Membranes were blocked overnight at 4 °C in Tris buffered saline (TBS) containing 20% goat serum and 5% bovine serum albumin (BSA). Membranes were then washed and incubated with anti-catalase polyclonal antibody or anti PRDX1 polyclonal antibody for 2 hrs at room temperature.

After washing, membranes were incubated with the appropriate secondary antibody conjugated to alkaline phosphatase for 1 hr at room temperature. Protein bands were developed with Sigma Fast NBT/BCIP (Sigma-Aldrich., St. Louis, MO).

Statistical analysis

Data were analyzed either by analysis of variance (ANOVA) or two sample t-test. Differences in which the p-value was less than 0.05 were considered statistically significant.

RESULTS

Cytopathic BVDV infection induces apoptosis in infected BT cells

In order to examine whether cell death in a BVDV infected BT cell line is due to apoptosis or necrosis, cells were stained with Annexin V and propidium iodide (PI) to measure apoptosis or necrosis, respectively. As shown in Figure 1A, NCP BVDV caused an increase in early apoptosis after 48 hrs of infection (lower right) compared to uninfected cells. On the other hand, both early and late (upper right) apoptotic changes were more apparent when cells were infected with CP BVDV. Cells treated with staurosporine for 1 hr mostly exhibited necrosis, as expected. Infection of BT cells with CP BVDV, but not with the NCP BVDV, resulted in a significant increase in apoptosis (early and late) in a time-dependent manner, as shown in Figure 1B. This suggests the increased activity of initiator caspases in CP BVDV-infected cells, which leads to the externalization of phosphatidylserine residues on the outer plasma membrane that is detected by Annexin V.

Involvement of mitochondrial membrane potential disruption and reactive oxygen species in cytopathic BVDV-induced apoptosis

To elucidate the involvement of mitochondria in the BVDV-induced apoptosis pathway, disruption of the mitochondrial membrane potential was investigated in BT cells. Changes in mitochondrial membrane potential following infection of BT cells with the two biotypes of BVDV were measured by flow cytometry using the DePsipherTM kit. Figure 2A shows a decrease in the ratio of orange (intact membrane) to green (disturbed membrane) florescence in BT cells due to CP BVDV compared
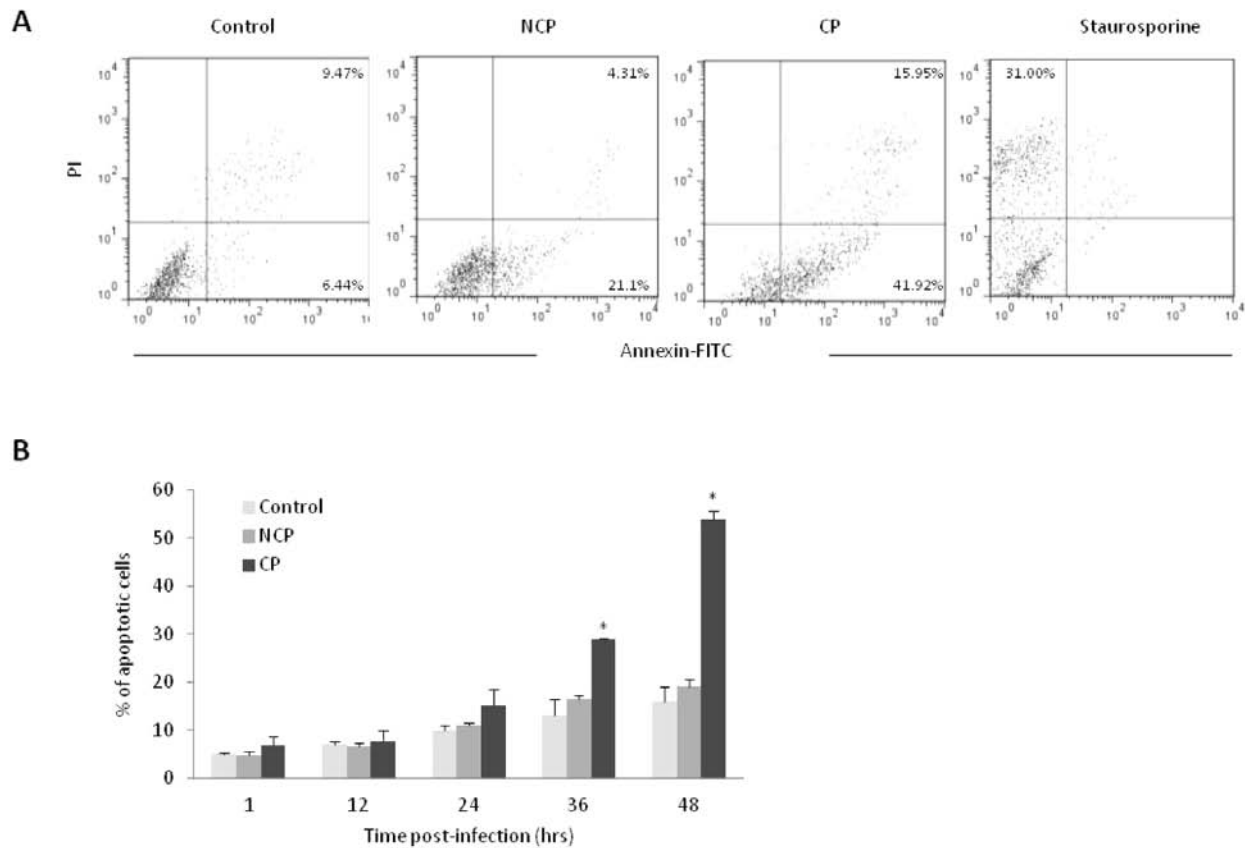
Figure 1. CP BVDV induce apoptosis in BT cells. BT cells were infected with CP or NCP BVDV at different time points. At the end of the each incubation period, cells were stained with Annexin V/PI for 10 min. Apoptotic cells were determined using flow cytometry as described in the materials and methods. A) BVDV-induced apoptosis at 48 hrs post infection, which are representative of two separate experiments. Live, early apoptotic, late apoptotic and necrotic cells are present in lower left, lower right, upper right and upper left quadrant, respectively. Uninfected cells and cells treated with staurosporine were used as a negative and positive control, respectively. This is one of two representative experiments. B) Kinetics of BVDV-induced apoptosis (early and late apoptotic) as percentages. Data are represented as mean $\pm$ SD of two independent experiments. *P < 0.05 as determined by the treatment *vs* control at each time point.

to NCP BVDV and uninfected cells. Treatment with staurosporine for 1 hr decreased the overall number of viable cells and increased the percentage of disrupted cells to 21%. Figure 2B shows the ability of CP BVDV to disrupt the mitochondrial membrane potential over time. The fraction of cells exhibiting green fluorescence became detectable at 1 hr post-infection, increasing with time to be significantly expressed after 36 and 48 hrs post CP BVDV infection reaching 13% and 16% compared to NCP BVDV, respectively. Interestingly, NCP BVDV showed a numerical increase in the green fluorescence in early infection that decreased with time compared to uninfected

levels. As alterations in the mitochondrial membrane potential have been shown to be one of the first intracellular changes following the onset of apoptosis, these results demonstrated that disruption of mitochondrial membrane potential was involved in CP BVDV-induced apoptosis.

Since enhanced electron leakage leading to ROS formation is a hallmark of defective activity in mitochondrial complexes, we next measured the intracellular ROS production in BT cells following viral infection. ROS production was determined using the carboxy-H_2DCFDA dye. The enhanced production of ROS in BT cells treated with H_2O_2 compared to uninfected control cells is shown in Figure 3A.
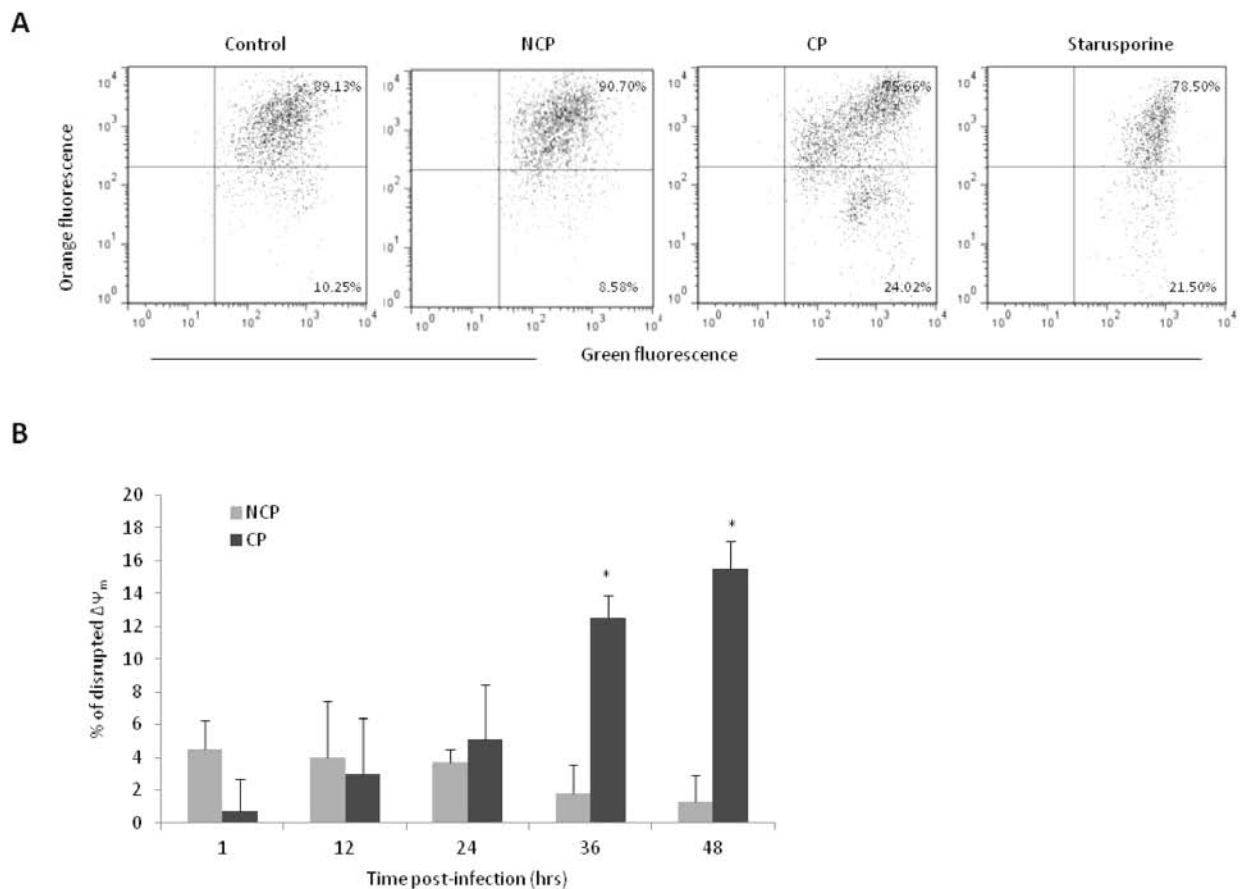
Figure 2. Change in the mitochondrial membrane potential after infection of BT cells with CP BVDV. At each time point infection, BT cells were stained with DePsipherTM for 20 min at 37 °C. A) $\Delta\Psi$m at 48 hrs post infection, which are representative of two separate experiments. The percentage of orange-red and green fluorescence represents intact and altered membrane potential, respectively. Cells treated with staurosporine were used as a positive control. This is one of two representative experiments. B) Kinetics of BVDV-induced changes in $\Delta\Psi$m expressed as % green fluorescence of BVDV-infected cells relative to uninfected cells of the respective time point. Data are represented as mean $\pm$ SD of two independent experiments. *$P < 0.05$ as determined by CP *vs* NCP BVDV at each time point.

CP BVDV-induced ROS production was apparent at 24 hrs and remained significantly elevated after 36 and 48 hrs post-infection compared to NCP BVDV (Figure 3B). On the other hand, NCP BVDV showed a slight decrease in ROS production compared to uninfected cells. These results showed that ROS is involved in CP BVDV-induced apoptosis and it correlated with the disruption in the mitochondrial membrane potential.

BVDV biotypes alter antioxidant enzymes involved in oxidative stress

Antioxidant enzymes are involved in cell defence against ROS production and oxidative stress [24].

Our proteomics data indicate that multiple antioxidant proteins were altered in bovine monocytes after 24 hrs infection with BVDV biotypes (Table 3). A difference between the two BVDV biotypes was shown with CP BVDV infection causing a down-regulation of catalase (CAT) and NCP BVDV up-regulated PRDX-1 and -5. To determine if BVDV biotype infections change the expression levels of antioxidant enzymes in BT cells, antibodies specific for CAT and PRDX1 were used for flow cytometry and western blot analyses. Figure 4A shows that both CP and NCP BVDV had a slight insignificant decrease in CAT expression, as determined by flow cytometry. Figure 4B shows an increase in

A

B
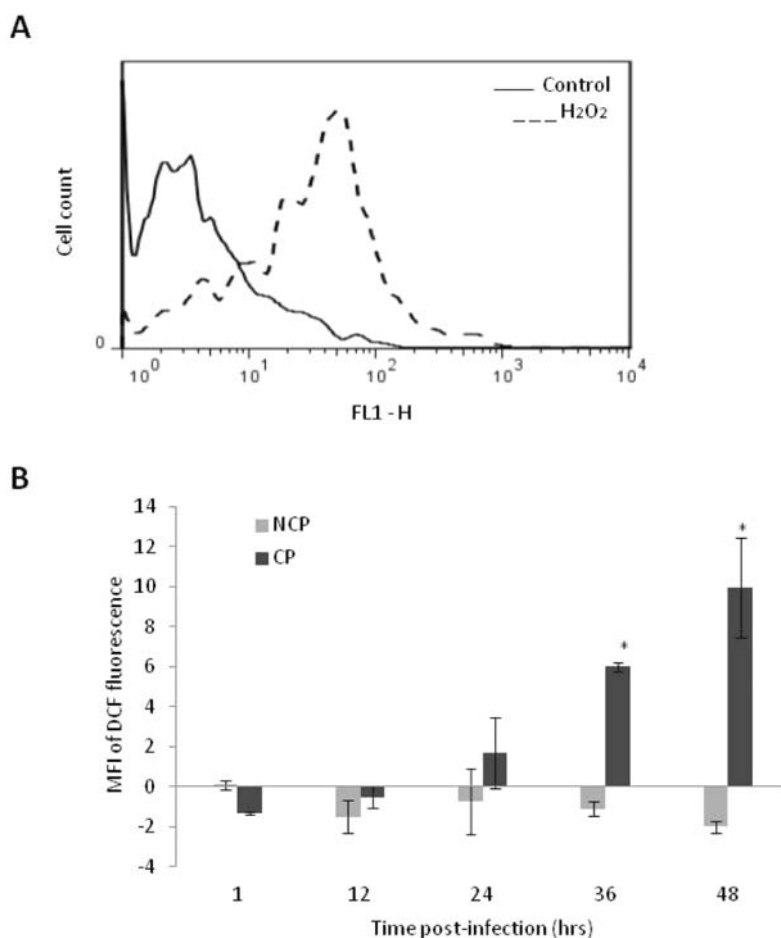
Figure 3. Intracellular ROS production by CP BVDV-infected BT cells. The intracellular ROS was measured by the quantification of carboxy-H2DCFDA fluorescence of viable cells as described in the materials and methods section. A) ROS production in H_2O_2-treated BT cells. Cells alone and in the presence H_2O_2 were used as negative and positive controls, respectively. This is one of the two representative experiments. B) Kinetics of BVDV-induced ROS production. The mean fluorescence intensity (MFI) was normalized to the uninfected controls of the respective time point. Data are represented as mean ± SD of two independent experiments. *$P < 0.05$ as determined by CP *vs* NCP BVDV at each time point.

PRDX expression at 12 hrs post NCP BVDV-infection that starts to decrease with time. However, PRDX levels were significantly lower for CP BVDV compared to NCP BVDV during early infection, but continued to increase over time such that PRDX was significantly higher than for NCP BVDV at 48 hrs. Western blot analysis did not show a significant change in CAT or PRDX1 between uninfected and BVDV-infected cells (data not shown).

DISCUSSION

The mitochondria are the major supplier of energy in the cells [25], which results from the metabolic sequence known as the tricarboxylic acid (TCA) cycle (also called citric acid cycle), coupled with the mitochondrial oxidative phosphorylation (OxPhos) system [26]. The OxPhos system is composed of five complexes: complex I (NADH dehydrogenase), complex II (succinate dehydrogenase), complex III (cytochrome *c* reductase), complex IV (cytochrome *c* oxidase) and complex V (ATP synthase) [27]. The coupling of complexes I, III and IV in the translocation of protons from the mitochondrial matrix to the intermembrane space generates a proton gradient that can be used by complex V to catalyze the formation of ATP by the phosphorylation of ADP [27]. Loss of OxPhos complexes functions
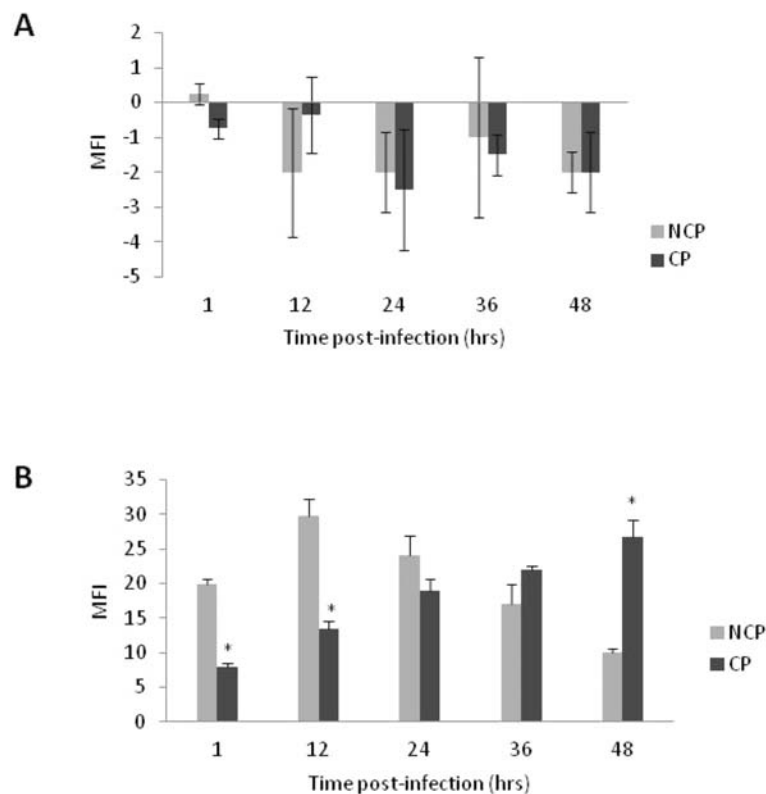
Figure 4. Effect of BVDV infection on catalase and PRDX levels in BT cells. Catalase and PRDX1 expression levels were measured by flow cytometry as described in material and methods. The expression levels of A) CAT and B) PRDX1 are at different time points shown as mean fluorescence intensity (MFI). The MFI was normalized to the uninfected controls of the respective time point. Data are represented as mean ± SD of two independent experiments. *P < 0.05 as determined by CP *vs* NCP BVDV at each time point.

is responsible for the decrease in ATP production, in addition to an increase in reactive oxygen species (ROS) causing mitochondrial damage [28].

Further analysis of differentially expressed host proteins from our previous proteomics study [20], shows that the top eight pathways involved in CP BVDV infection are as follows; mitochondrial dysfunction, propanoate metabolism, valine, leucine and isoleucine degradation, pyruvate metabolism, citrate cycle, butanoate metabolism, oxidative phosphorylation (OxPhos) and fatty acid metabolism (Table 1). Our results demonstrate that the "mitochondrial function pathways" were the most affected pathways following CP BVDV infection with an overall down-regulation of proteins involved in these pathways [20]. Twenty-four hours post-infection of monocytes with CP BVDV decreased the expression of two pyruvate dehydrogenase (PDH) subunits (PDHA1 and

PDHB), multiple acetyl-coenzyme A (acetyl CoA) and other enzymes required for the appropriate function of pyruvate metabolism and the TCA cycle. The conversion of pyruvate to acetyl CoA by PDH complex is required for the generation of NADH and FADH that carries electrons to the OxPhos complexes. Here, CP biotype infection down-regulated host proteins in four complexes of the OxPhos system (Table 2). Complex I is a major source of ROS in mitochondria and its deficiencies are identified across a wide spectrum of pathologies and linked to enhanced superoxide production as well as to deficiencies in energy production [29]. ROS is known to be an inhibitor of OxPhos complex I and IV [30, 31] and thus can cause the production of more harmful ROS. Previous studies showed that the pro-inflammatory cytokine TNF-α mediated an early inhibitory effect on the OxPhos system, specifically complex IV [32], during

CP BVDV-infection [33]. Based on the above considerations, we speculate that by dysregulating cellular proteins involved in the OxPhos complexes, CP BVDV contributes to $\Delta\Psi$m breakdown and uncoupled respiration, which consequently leads to oxidative stress-induced apoptosis.

In contrast to the CP biotype, proteomics analysis showed fewer proteins were affected by the NCP biotype (Table 2). In the OxPhos pathway, the NCP BVDV up-regulated two proteins (ATP6V1A and NDUFB7); however, CP also had similar effect on those proteins probably due to the fact that both CP and NCP biotypes are antigenically related. Interestingly, in the mitochondrial dysfunction pathway, NCP infection is shown to up-regulate the uncoupling protein 2 (UCP2) (Table 1). Previous studies supported the existence of uncoupling activity in UCP2, defining it as a protein devoted to the limitation of ROS [34, 35]. The up-regulation of UCP2 by NCP suggests its role as an antioxidant defence mechanism. In addition, NCP biotype infection up-regulated the expression level of PARP1, a nuclear enzyme involved in DNA repair [18] which could be an important factor contributing to the development of persistent infection. These results indicate that the NCP biotype is either not using the intrinsic pathway of apoptosis or is inhibiting this pathway.

Previously, Grummer *et al.* suggested the role of mitochondria in the BVDV-1-induced apoptosis of FBK cell line based on the evidence that incubation of these cells with mitochondrial permeability transition pore (MPTP) inhibitors delayed the cytopathic effect of BVDV-1 [15]. In addition, it was shown that generation of ROS is a prominent feature of BVDV-induced apoptosis [12]. Finally, the protein expression data by Jordan *et al.* and our proteome analysis showed the involvement of multiple mitochondria-related proteins in BVDV-induced apoptosis [14, 20]. Based on these observations and since a hallmark of defective activity in mitochondrial proteins is an enhanced electron leak leading to ROS production [36], we used a kinetic analysis to measure changes in those parameters over time. An increase in ROS and breakdown of $\Delta\Psi$m were apparent in bovine peripheral blood monocytes. However, due to a considerable variation between individual animals the observed changes were not significant (data not shown). We used the embryonic BT cell line to assess if the decreases in the protein expression seen in monocytes also occur in other cell types susceptible to BVDV infection. Our studies indicate that the cytopathic effect exerted in BT cells with CP BVDV was attributed to induced apoptosis in a time-dependent manner. With BT cells, the disruption of $\Delta\Psi$m started at 1 hr post CP BVDV infection and reached a significant level at 48 hrs. The collapse of $\Delta\Psi$m observed suggest that CP BVDV-infected cells have a diminished oxidative phosphorylation capacity, as shown in monocytes through the decrease of proteins involved in mitochondrial functions. As a consequence of $\Delta\Psi$m breakdown, cytochrome *c* is released into the cytoplasm and it binds to apaf-1. Release of cytochrome *c* and increase in the amount of apaf-1 in the cytosol as a consequence of $\Delta\Psi$m breakdown, following CP BVDV infection has been previously demonstrated [15]. To determine if ROS is a consequence or is inducing the observed $\Delta\Psi$m changes, we next measured ROS formation. The increase in ROS levels at 24 hrs accompanied the increase in apoptotic cells and preceded the sign of $\Delta\Psi$m breakdown in cells infected with CP BVDV compared to uninfected cells. This can indicate that ROS generation was a result of mitochondrial dysfunction. Overall, compared to ROS levels, changes in the $\Delta\Psi$m started earlier showing an increase above the uninfected control levels at 1 hr post CP BVDV-infection.

To counteract ROS, cells contain numerous antioxidant defence systems. Hydrogen peroxide (H_2O_2) is one of the major ROS in the cells. One of the primary antioxidant enzymes converting H_2O_2 into harmless compounds is CAT, which cannot be saturated by H_2O_2 at any concentration [37]. With proteomics data, the loss of CAT activity in cells infected with CP BVDV biotype could increase oxidative stress which contributes to the mechanisms of apoptosis. However, with BT cells, no significant change was detected with flow cytometry or Western blot at any time point. In addition, proteomics analysis showed that the two isoforms of PRDX, PRDX-5 and -1, are up-regulated by NCP BVDV infection. This increase was seen also with PRDX1 using flow cytometry, which peaked at 12 hrs post-infection. The relative abundance of PRDX1 appears to protect cells from

harmful levels of H_2O_2 [38]. This increase also occurs with CP BVDV infection in a time-dependent manner, indicating a compensatory mechanism to eliminate oxidative stress. The differences between the proteomics, flow cytometry and Western blot results may be due to cell type differences and/or the sensitivity of the experimental approach used. The BT cells were not found to produce nitric oxide or peroxynitrite [12], two forms of ROS, suggesting that peroxidase is responsible for ROS production in CP BVDV infection. This indicates that different antioxidants respond to different ROS produced in monocytes and BT cells.

CONCLUSION

Proteomics analysis show that monocytes exposed to CP BVDV for 24 hrs exhibited strong down-regulation of proteins involved in mitochondria and OxPhos system. The direct damage to mitochondrial proteins decreases their function and contributed to $\Delta\Psi$m breakdown and the hyperproduction of ROS seen in BT cells infected with CP BVDV, but not with NCP BVDV. This finding indicates that the CP biotype, but not the NCP biotype, induces oxidative stress apoptosis mediated by mitochondrial dysfunction in both cell types. Also, our proteomics study shows that CP BVDV infection contributed to oxidative stress by the disturbance of cellular antioxidants system. However, our work here with the transformed BT cell line demonstrates that the antioxidant enzyme that contributes to mitochondrial dysfunction is different between monocytes and BT cells, suggesting that BVDV is capable of manipulating multiple antioxidant enzymes. We also show evidence of the involvement of OxPhos system in CP BVDV-dependent mitochondrial dysfunction. Overall, our data not only confirm the previous *in vitro* observations on the association of the intrinsic pathway of apoptosis in CP BVDV infection [12, 15], but also identify mitochondrial and antioxidant proteins contributing to this pathway. The expression and function of the proteins involved in this pathway will be the subject of further investigations.

CONFLICT OF INTEREST STATEMENT

The authors declare that they have no competing interests.

ABBREVIATIONS

BVDV, Bovine Viral Diarrhea Virus; CP, cytopathic; NCP, non-cytopathic; OxPhos, oxidative phocphorylation; $\Delta\Psi$m, mitochondrial membrane potential; CAT, catalase; PRDX1, peroxiredoxin1; ROS, reactive oxygen species; MPTP, mitochondrial permeability transition pore; FBK, fetal bovine kidney; MBDK, Madin-Darby Bovine Kidney; PBMC, peripheral blood mononuclear cells, IPA, Ingenuity Pathway Analysis; BT, bovine turbinate

REFERENCES

1. Marianneau, P., Cardona, A., Edelman, L., Deubel, V. and Despres, P. 1997, J. Virol., 71, 3244.
2. Takizawa, T., Matsukawa, S., Higuchi, Y., Nakamura, S., Nakanishi, Y. and Fukuda, R. 1993, J. Gen. Virol., 74, 2347.
3. Fugier-Vivier, I., Servet-Delprat, C., Rivailler, P., Rissoan, M. C., Liu, Y. J. and Rabourdin-Combe, C. 1997, J. Exp. Med., 186, 813.
4. De Luca, A., Bugarini, R., Lepri, A. C., Puoti, M., Girardi, E., Antinori, A., Poggio, A., Pagano, G., Tositti, G., Cadeo, G., Macor, A., Toti, M. and D'Armino Monforte, A. 2002, Arch. Intern. Med., 162, 2125.
5. Jaruga, P. 1999, Postepy. Hig. Med. Dosw., 53, 43.
6. Piccoli, C., Scrima, R., D'Aprile, A., Ripoli, M., Lecce, L., Boffoli, D. and Capitanio, N. 2006, Biochim. Biophys. Acta., 1757, 1429.
7. Soundravally, R., Sankar, P., Bobby, Z. and Hoti, S. L. 2008, Platelets, 19, 447.
8. Schwarz, K. B. 1996, Free Radic. Biol. Med., 21, 641.
9. Brownlie, J., Clarke, M. C., Howard, C. J. and Pocock, D. H. 1987, Ann. Rech. Vet., 18, 157.
10. Houe, H. 1987, Vet. Microbiol., 64, 89.
11. Schweizer, M. and Peterhans, E. 2001, J. Virol., 75, 4692.
12. Schweizer, M. and Peterhans, E. 1999, J. Gen. Virol., 80, 1147.
13. Zhang, G., Aldridge, S., Clarke, M. C. and McCauley, J. W. 1996, J. Gen. Virol., 77, 1677.
14. Jordan, R., Wang, L., Graczyk, T. M., Block, T. M. and Romano, P. R. 2002, J. Virol., 76, 9588.

15. Grummer, B., Bendfeldt, S., Wagner, B. and Greiser-Wilke, I. 2002, Virus Res., 90, 143.
16. Elmore, S. 2007, Toxicol. Pathol., 35, 516.
17. Karbowski, M. and Youle, R. J. 2003, Cell Death Differ., 10, 870.
18. Grummer, B., Bendfeldt, S. and Greiser-Wilke, I. 2002, J. Vet. Med. B. Infect. Dis. Vet. Public Health, 49, 298.
19. Lambot, M., Hanon, E., Lecomte, C., Hamers, C., Letesson, J. J. and Pastoret, P. P. 1998, J. Gen. Virol., 79,1745.
20. Ammari, M. G., McCarthy, F. M., Nanduri, B. and Pinchuk, L. M. 2010, BMC Bioinformatics, 11, 59.
21. Lee, S. R., Nanduri, B., Pharr, G. T., Stokes, J. V. and Pinchuk, L. M. 2009, Biochim. Biophys. Acta, 1794, 14.
22. Pan, J., Chang, Q., Wang, X., Son, Y., Zhang, Z., Chen, G., Luo, J., Bi, Y., Chen, F. and Shi, X. 2010, Chem. Res. Toxicol., 23, 568.
23. Jiang, Y., Guo, C., Vasko, M. R. and Kelley, M. R. 2008, Cancer Research, 68, 6425.
24. Bai, J., Rodriguez, A. M., Melendez, J. A. and Cederbaum, A. I. 1999, J. Biol. Chem., 274, 26217.
25. Dudkina, N. V., Sunderhaus, S., Boekema, E. J. and Braun, H. P. 2008, J. Bioenerg. Biomembr., 40, 419.
26. Pieczenik, S. R. and Neustadt, J. 2007, Exp. Mol. Pathol., 83, 84.
27. Boekema, E. J. and Braun, H. P. 2007, J. Biol. Chem., 282, 1-4.
28. Kadenbach, B., Ramzan, R., Wen, L. and Vogt, S. 2009, Biochim. Biophys. Acta, 1800, 205.
29. Kussmaul, L. and Hirst, J. 2006, Proc. Natl. Acad. Sci. USA, 103, 7607.
30. Jekabsone, A., Ivanoviene, L., Brown, G. C. and Borutaite, V. 2003, J. Mol. Cell. Cardiol., 35, 803.
31. Shiva, S. and Darley-Usmar, V. M. 2003, IUBMB Life, 55, 585.
32. Samavati, L., Lee, I., Mathes, I., Lottspeich, F. and Huttemann, M. 2008, J. Biol. Chem., 283, 21134.
33. Yamane, D., Nagai, M., Ogawa, Y., Tohya, Y. and Akashi, H. 2005, Microbes Infect., 7, 1482.
34. Fleury, C., Neverova, M., Collins, S., Raimbault, S., Champigny, O., Levi-Meyrueis, C., Bouillaud, F., Seldin, M. F., Surwit, R. S., Ricquier, D. and Warden, C. H. 1997, Nat. Genet., 15, 269.
35. Diehl, A. M. and Hoek, J. B. 1999, J. Bioenerg. Biomembr., 31, 493.
36. Suen, D. F., Norris, K. L. and Youle, R. J. 2008, Genes Dev., 22, 1577.
37. Karabullutesn, A. B., Sonmez, E., Bayindir, Y. and Gozokara, E. 2001, Turk. J. Med. Sci., 32, 313.
38. Rhee, S. G., Chae, H. Z. and Kim, K. 2005, Free Radic. Biol. Med., 38, 1543.